

## PATTERNED DEPOSITION OF ALLOPHANE NANOPARTICLES ON SILICON SUBSTRATES

MARCO FUCHS<sup>1</sup>, ZAENAL ABIDIN<sup>2,3</sup>, CHRISTIAN KÜBEL<sup>4</sup>, PETER G. WEIDLER<sup>1</sup>, NAOTO MATSUE<sup>2</sup>, TERUO HENMI<sup>2</sup>, RAINER KÖSTER<sup>1,5</sup>, AND HARTMUT GLIEMANN<sup>1,\*</sup>

<sup>1</sup> Institute of Functional Interfaces (IFG), Karlsruhe Institute of Technology (KIT) Campus North, Hermann-von-Helmholtz-Platz 1, 76344 Eggenstein-Leopoldshafen, Germany

<sup>2</sup> Faculty of Agriculture, Ehime University Tarumi, 3-5-7, Matsuyama, Ehime Prefecture, 790–8566 Japan

<sup>3</sup> Department of Chemistry, Faculty of Natural Science and Mathematics, Bogor Agricultural University, Kampus Darmaga, Bogor, West of Java, Indonesia

<sup>4</sup> Institute of Nanotechnology (INT), Karlsruhe Institute of Technology (KIT) Campus North, Hermann-von-Helmholtz-Platz 1, 76344 Eggenstein-Leopoldshafen, Germany

<sup>5</sup> Institute of Analytical Chemistry, Chemo- and Biosensors, University of Regensburg, Universitätsstraße 31, 93053 Regensburg, Germany

**Abstract**—In order to obtain nanopatterned surfaces, natural allophane particles originating from Japanese soils were immobilized as single particles on Si wafer substrates. When derived from aqueous suspensions, only a few nanoparticles were deposited and detected on the surface due to the weak adsorption of allophanes on the substrate. The amount of immobilized allophane was increased significantly, however, by using an organic solvent in combination with a micelle-based technique to suspend the allophane particles. The micelles were formed from a tailored, aliphatic diblock copolymer that was dissolved in toluene and contained several allophane particles. A cleaned silica chip was used as a substrate on which a monolayer of micelles was immobilized equidistant from each other by dip coating. To remove the polymer from the substrate and to produce free, single allophane nanoparticles, ultraviolet (UV) irradiation was used. After UV treatment, single allophane particles formed ring-shaped deposition patterns with a high surface density. Transmission electron microscopy (TEM) was used to verify the presence of single allophane nanoparticles in the Japanese samples which came from natural sources. The single allophane particles as well as the allophane-containing di-block copolymer micelles, both immobilized on Si substrates and TEM sample grids, were imaged by atomic force microscopy and TEM. In this way, the diameters of the single allophane particles, as well as the distances between the immobilized micelles and the particles and their topography on the substrates, were determined.

**Key Words**—AFM, Allophane, Diblock Copolymer, Micelle, Nanoparticle, Nanostructuring.

### INTRODUCTION

Nanostructured surfaces have become very important for many technical, biological, and medical applications (Onodera *et al.*, 2001; Lipski *et al.*, 2007). Structures based on immobilized, chemically modified nanoparticles with diameters <10 nm are used to promote, for example, the attachment of cells to substrate interfaces. The attachment behavior of the cells depends on different parameters such as particle size and particle density on the substrate. Nanoparticles can be used directly as the structure-forming building blocks (Glass *et al.*, 2003) but they also can be used as masks or precursors for the preparation of nanostructures (Manzke *et al.*, 2007). Research in this field, therefore, requires particles with a well defined and narrow size distribution and geometry, and with a reactive surface. Although possible, the synthesis of particles with these properties

is challenging, time-consuming, and expensive. An alternative, low-cost approach is suggested here which is based on the use of natural, oxidic, hollow allophane nanoballs as building blocks for nanostructured surfaces. These natural particles possess some remarkable characteristics making them an excellent, low-cost material.

Allophanes are hollow, spherical, nanosized silicate particles which have a narrow size distribution with diameters ranging from 3.5 to 5 nm (Henmi and Wada, 1976; Creton *et al.*, 2008). They exhibit six pores which are arranged in pairs perpendicular to each other (Abidin *et al.*, 2007a) and provide limited chemical access to their inner parts, offering a chemical environment that differs from that of the outer surface. The allophane particles carry OH groups on the inner and on the outer interfaces which have different dissociation values, and which can be used for sorption processes or chemical reactions (Abidin *et al.*, 2007b). Allophane nanoballs have a well defined crystalline order (Kaufhold *et al.*, 2009) and a defined size and shape, though little use has been made of them for technical purposes or for sophisticated applications, *e.g.* as nanosized containers or binding sites. Steps in that direction include the

\* E-mail address of corresponding author:

hartmut.gliemann@kit.edu

DOI: 10.1346/CCMN.2012.0600502

application of allophane particles as building blocks for films formed at the liquid–liquid interface (Watanabe *et al.*, 2009), as a catalyst for the decomposition of hemicellulose (Ogaki *et al.*, 2011) or trichloroethylene (Nishikiori *et al.*, 2011), or as one component of humidity-controlling ceramic composite materials (Vu *et al.*, 2011). Allophanes may be sourced from natural deposits or through synthesis (Abidin *et al.*, 2007a).

The purpose of the present study was to assess whether an innovative micelle-based method can be established: (1) to extract single allophane nanoparticles from cheap allophane bulk material in an organic solvent; and (2) to immobilize the allophane nanoparticles on the surface of Si wafers in a patterned way by dip coating. Such a method would be an important proof of concept for future applications, where allophane nanoballs deposited site-selectively could be used as inorganic, reactive, and biocompatible centers, which could then be chemically functionalized in a selective manner to create nanosized centers for specific adhesion, *e.g.* for proteins or biological cells. The patterning described here was achieved by the deposition of an allophane-containing micelle consisting of a diblock copolymer (Lohmueller *et al.*, 2008) which is able to enclose allophane particles and carry them from an aqueous into an organic solution. Transmission and scanning transmission electron microscopy (TEM and STEM) as well as atomic force microscopy (AFM) were used to characterize the allophane material and the surfaces prepared by investigating the particle diameters and distances between the particles deposited.

## MATERIALS AND METHODS

### *Treatment of raw material*

Weathered pumice, collected from Mount Daisen in Kurayoshi, Tottori Prefecture, Japan, referred to below as KyP, was used as a natural material for the experiments. The outer parts of the weathered pumice were scraped off in water to obtain a clay sample free of imogolite, glass, opaline silica, and other contaminants. The weathered pumice sample was ground carefully in the presence of water to prevent alteration of allophane and then sonified using an ultrasonic homogenizer at 28 kHz for ~5 min. The sonified suspension was then transferred into a 1 L cylinder and the suspended samples were adjusted to pH 4 using diluted (3.5% vol.) HCl (Merck, Darmstadt, Germany) to facilitate dispersion because of their large Al contents. The samples were then stoppered, shaken reciprocally by hand, and allowed to stand overnight for sedimentation of the silt- and sand-size fractions. The pipette method was used to separate the clay fraction while the silt- and sand-size fractions were discarded. The fine clay fraction (<0.2  $\mu\text{m}$ ) was separated by centrifugation of the flocculated clay sample after adjustment to pH 4. This process was repeated twice to ensure recovery of

most of the <0.2  $\mu\text{m}$  fraction. The clay fraction collected was flocculated and washed free of NaCl several times with water by dialysis. To guarantee purity, the samples were freeze dried and subjected to X-ray diffraction (XRD), infrared spectroscopy, and differential thermal analysis (results not shown here, but see Henmi and Wada, 1976; Karube *et al.*, 1996). Chemical and mineralogical analysis revealed that the sample was a pure allophane with nanoball morphology and with a Si/Al ratio of 0.67 for the single particles extracted. The Si/Al ratio was determined by the acid oxalate method (Higashi and Ikeda, 1974). The purified material is referred to hereafter as KyP base material.

### *Sample preparation*

As substrates for particle immobilization, 1-cm<sup>2</sup> pieces of a Si (100) wafer (26/10CPBW/9,00./525, Silchem, Freiberg, Germany) were used. Prior to particle deposition, the Si substrates were: (1) cleaned in boiling piranha solution consisting of concentrated (95.0–98%) H<sub>2</sub>SO<sub>4</sub> (Sigma-Aldrich, St. Louis, Missouri, USA), 35% H<sub>2</sub>O<sub>2</sub> (Merck, Darmstadt, Germany), and deionized water at a volume ratio of 1:1:5; and (2) irradiated by UV (MHL 570, UV-Technik Meyer GmbH, Ortenberg, Germany) to remove organic carbon.

Two methods were used for particle immobilization.

(1) Extraction of single allophane particles from the KyP base material in an aqueous suspension: 2 mg of the freeze-dried allophane powder was suspended in deionized water, giving a concentration of 2 mg/mL, and dispersed by ultrasonication for 15 min. Afterward, the resulting suspension was centrifuged for 3 h at 43,000  $\times$  g. The supernatant was collected and a freshly cleaned Si substrate was dipped into the supernatant.

(2) Preparation of micelle-stabilized allophane material (Figure 1): the diblock copolymer, poly(styrene-*b*-2-vinyl)pyridine (PS–P2VP) from Polymer Source, Inc. (Dorval, Quebec, Canada) was used for the micelle preparation, with average molar masses of 213,000 g/mol for the polystyrene block and 206,000 g/mol for the pyridine block (Figure 1a). For each sample, 20 mg of PS–P2VP was dissolved in 1 mL of toluene (Xie and Blum, 1996a, 1996b), 2 mg allophane powder was added subsequently and dispersed by means of an ultrasonic treatment, until the polymer was dissolved completely (Figures 1b–c). The resulting solutions were centrifuged for 3 h at 43,000  $\times$  g and the supernatants were collected. Afterward, a freshly cleaned Si substrate was dipped into the supernatant and dried with nitrogen (Figure 1d–e). The samples were then investigated using AFM.

After the immobilization of the micelle-stabilized allophanes (Xie and Blum, 1996a, 1996b), a UV lamp (MHL 570, UV-Technik Meyer GmbH, Ortenberg, Germany) with an emission maximum between 250 and 400 nm, mounted in a home-built irradiation apparatus and working under ambient conditions, was

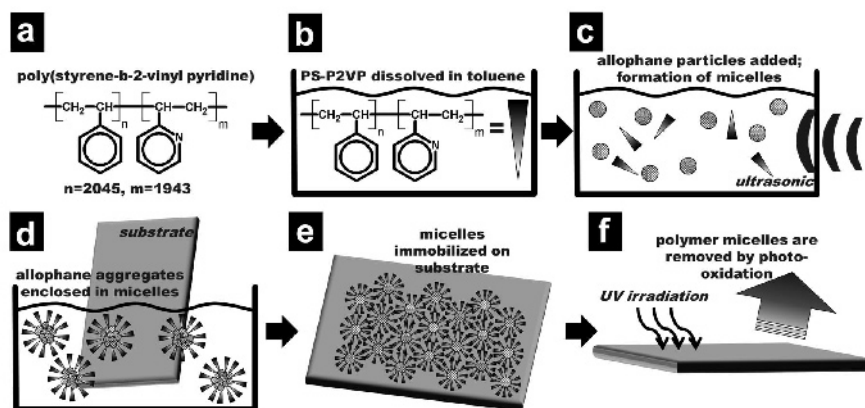


Figure 1. Preparation process for allophane-based, nanostructured Si substrates with the help of PS–P2VP (a–f). For (d) the supernatant of sample (c) after centrifugation was used.

used to remove redundant polymer from the samples (Figure 1f). By applying exposure times of 5 to 30 min, oxidation effects at the air–sample interface were utilized to destroy the polymer, without causing damage or displacement of the allophane particles (Lohmueller *et al.*, 2008). For the irradiation, the distance between the light source and the sample surface was kept constant at 20 cm.

For TEM and STEM investigations the samples were prepared on 300 mesh copper grids (HC 300 CU) coated with holey carbon film (25 ct) from Science Services (Munich, Germany). The allophane samples were applied either as an aqueous suspension (dispersed by an ultrasonic treatment, centrifuged, dropped onto a grid, and dried at 60°C) or as a freeze-dried powder.

#### Instruments used for characterization

Investigations by TEM and STEM were recorded using an image-corrected Titan 80–300 (FEI, Hillsboro, Oregon, USA) transmission electron microscope at an acceleration voltage of 300 kV. For STEM, a nominal spot size of 0.135 nm was used for imaging with a high-angle annular dark-field (HAADF) detector. For bright-field (BF) TEM imaging, the information limit is 0.8 Å and a Gatan US1000 slow-scan CCD camera was used for image acquisition. Images in both the TEM and STEM modes were acquired under (semi) low-dose conditions.

Atomic force microscopy was performed by using a multimode AFM from Digital Instruments (DI, Santa Barbara, California, USA), equipped with a Nanoscope IIIa-controller. A silicon chip (NSC35/no Al) from Mikromasch (San Jose, California, USA) was used in intermittent contact mode for imaging. The cantilever chip for AFM investigation comes with three cantilevers of different lengths. For the present study, cantilever C, 130 µm long, with a typical resonant frequency of 150 kHz and a force constant of 4.5 N/m, was applied. The radius of curvature of the tip was

<10 nm and the full tip cone angle was <30°. The AFM images recorded were evaluated and illustrated with NanoScope® III software, version 5.30r1.

## RESULTS AND DISCUSSION

#### KyP base material

In order to verify the presence of individual allophane spherules in the KyP base material, TEM was used. As the allophanes are hollow spherules (Abidin *et al.*, 2007a), they were observed as rings in the (S)TEM projections. The allophanes tended to accumulate and form large aggregates, but single allophane particles could be observed at the edges of the aggregates (Figure 2), where they were projected as circular structures from hollow spherules with an outer diameter of 4–5 nm (insets in Figure 2a and 2b). The allophane particles were quite sensitive to electron beam irradiation at 80 kV and 300 kV and imaging them required working under semi low-dose conditions. The BF-TEM image (Figure 2a) shows Fresnel rings around the allophane spherules due to the defocus used in the image, whereas the bright rings in the low-dose high-angle annular dark-field (HAADF) STEM image of the allophane aggregate (Figure 2b) represent directly the shells of the allophanes. Overall, both the TEM and STEM analysis show that the KyP base material consisted of aggregates of single allophane particles (Woignier *et al.*, 2008).

#### Allophane particles and micelles

Atomic force microscopy was used to investigate the single allophane particles which were deposited on a Si wafer from the aqueous suspension. Several single allophane particles distributed over the Si surface are shown on the topography image of the sample (Figure 3a). The diameter of the particles determined by AFM was between 12 and 18 nm. These values for single allophane particles were much greater than those

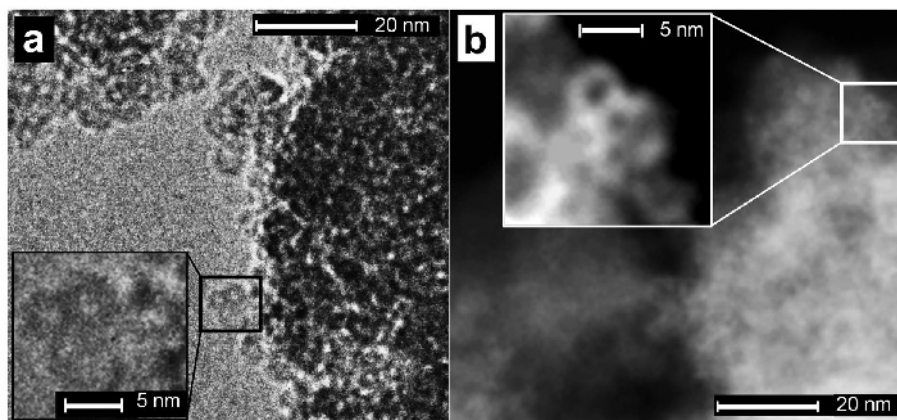


Figure 2. BF-TEM (a) and HAADF-STEM (b) images of KyP allophane agglomerates. The insets show individual allophane particles at the edge of the agglomerates.

determined by electron microscopy in Figure 2 or in the literature (Henmi and Wada, 1976), where diameters of between 3 and 5 nm were observed. This discrepancy in the diameters observed by AFM and electron microscopy is due to ‘tip convolution’ which is a known artifact of the AFM technique (Villarrubia, 1997). The relevance of tip convolution becomes increasingly more significant for smaller features investigated by AFM. The extent to

which tip geometry distorts the lateral size determined by AFM is shown in Figure 3c. During the scan of the AFM tip across the surface, the lateral force applied to the surface by the AFM tip is predefined and kept constant as a set point by a feedback system which controls the z-position of the sample. As soon as the flank of the conical AFM tip reaches the surface feature, the feedback system registers an increased lateral force

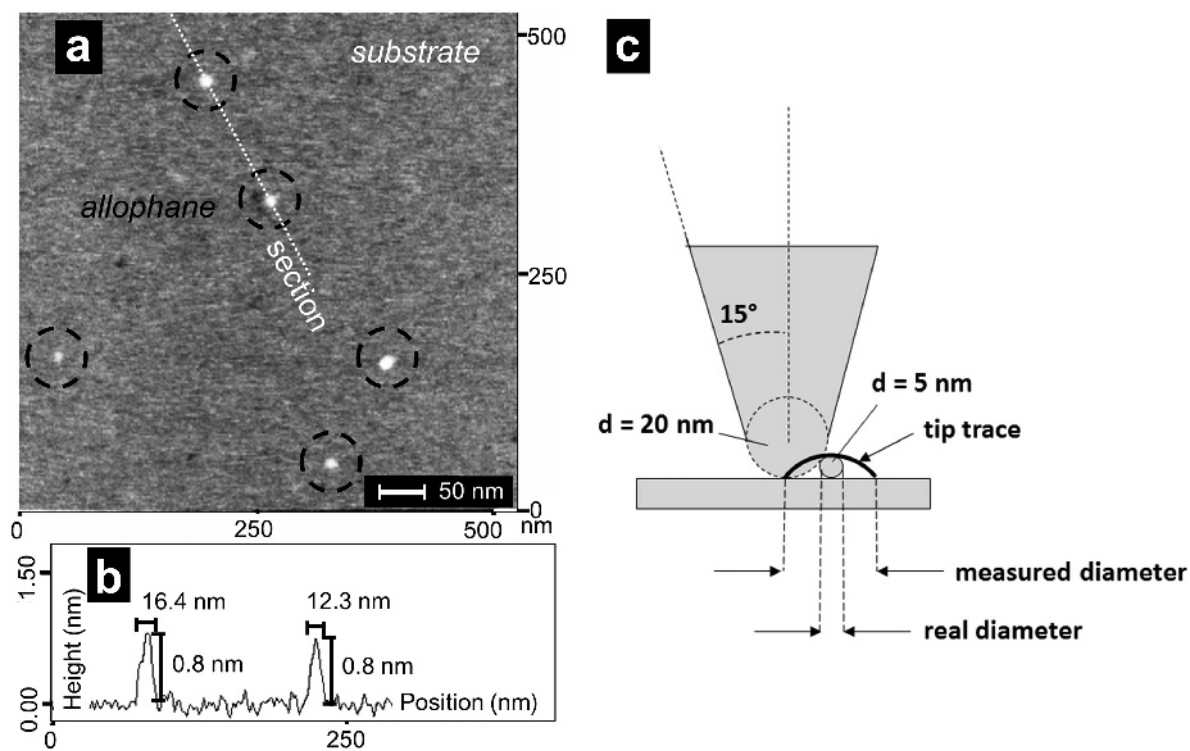


Figure 3. AFM topography image of single allophane particles marked with black circles, which are deposited on a Si wafer surface (a); (b) cross section along the white line in (a); (c) schematic representation of the influence of AFM tip convolution on the diameter of the nanoparticle determined: The geometrical conditions are depicted realistically and the error of measurement is >100%, as is obvious from the tip trace.



between the AFM tip and the surface. As a result, the sample is moved down so that the AFM tip can follow the topography of the feature without abrading or scratching material off. After the AFM tip apex reaches the highest point of the feature, the sample is lifted again for further scanning with the AFM tip at the defined set point force. The trace of the AFM tip apex is shown in Figure 3c. The distance between the left and the right intersection point of the tip trace and the substrate surface represents the lateral size of the particle determined by the AFM, which is not in accordance with the real size of the particle. This discrepancy depends heavily on the tip geometry, *e.g.* on the curvature radius of the tip apex and the opening angle of the tip. The difference between the real diameter and that determined by the AFM of a particle with a diameter of 5 nm is calculated by a simple geometrical model (Figure 3c). At a curvature radius of the applied AFM tip between 7 and 9 nm and an opening angle of 30°, a particle diameter of between 16 and 18 nm will be observed for an allophane particle using AFM. This simple model is in agreement with the results from the cross section shown in Figure 3b, where the diameters observed correlate with the expected, real diameter of 3.5–5 nm, when taking the tip convolution into account. However, as the measured height of the particles of ~1 nm (Figure 3b) was small compared to the expected allophane height of 3–5 nm (Henmi and Wada, 1976), a flattening of the particle due to the interaction of the allophane particles with the Si substrate and the AFM tip cannot be excluded, as demonstrated by Kaufhold *et al.* (2009).

The results here show that single allophane particles can be removed from the aqueous suspension of the KyP base material. With an average surface density of 16 particles per  $\mu\text{m}^2$  (Figure 3a), counted manually for three different samples, however, the yield of immobilized particles on the substrate was very small. According to the findings of the subsequent experiments, this low surface density was not the result of a low concentration of allophane nanoparticles in the suspensions used but instead due to the resulting low attractive interaction between the polar allophane particles and the less polar silicon wafer surface. Moreover, experiments performed under identical experimental conditions always revealed single allophane particles on the surface and no aggregates of particles were detected.

To increase the particle density on the surface, an alternative approach was developed. Here, toluene was used as a suspension agent instead of water and the diblock copolymer PS–P2VP was applied as a stabilizing agent. PS–P2VP is an amphiphilic molecule with both a hydrophobic and a hydrophilic block. Consequently, the molecules form micelles with the hydrophobic polymer block looking outside the micelle into the toluene. The micelles can carry hydrophilic material such as inorganic particles (Sikora and Tuzar,

2004). With these properties of the polymer, the inorganic allophanes could be dispersed in an organic solvent. The PS–P2VP acts both as a carrier of the particles and as a spacer between them to avoid aggregation in suspension as well as during the drying process on the substrate after dip coating. As the outer part of the micelles consists of the hydrophobic part of the diblock copolymer, adhesive interaction between the micelles and the Si wafer surface was much greater than in the case of the allophanes immobilized from the aqueous suspension (Lohmueller *et al.*, 2008).

After sample preparation (Figure 1), the immobilized, nanoparticle-containing micelles were investigated by AFM using a set of two different samples. The topography image of the sample (Figure 4a) shows a representative section of an island formed by a closely packed monolayer of allophane-filled PS–P2VP micelles on a Si wafer surface. The equidistant immobilization of the micelles was accomplished by hydrophobic polymer brushes on the outer side. The micelles were kept at constant distance according to the chain length of the polymer (Lohmueller *et al.*, 2008).

The spaces between the centers of the micelles ranged from 120 to 140 nm, their diameter being ~110 nm (base to base), including the surrounding polymer (Figure 4b). The island had an average height of 65 nm relative to the substrate surface. The TEM image presented (Figure 4c) shows diblock copolymer micelles forming an aggregate with a regular, closely packed arrangement on the carbon film of the sample grid. The micelles had a diameter and a center-to-center distance similar to those shown in the AFM image (Figure 4a), thus confirming that they are able to consistently structure a substrate. The dark rings in Figure 4c represent the polymer layer of the micelles ~30 nm thick, while the bright center has a diameter of ~80 nm. To prove that the micelles contain inorganic allophane particles, gradual UV treatment in air was carried out to remove the PS–P2VP by photo oxidation, and the samples were irradiated in steps of 5 min. The AFM topography image in Figure 5a shows an island consisting of micelles after 10 min of UV treatment. In contrast to the non-irradiated island (Figure 4a), the polymer layers around the elevated micelle centers were 6–20 nm tall relative to the substrate surface (Figure 5b). However, the closely packed structure of the island was still visible and the center-to-center distance among the micelles of 120–140 nm (Figure 5a) remained constant. The lateral expansion of the elevated structures (Figure 5a) had a diameter of 50–60 nm, which is too big for a single allophane particle, even if tip convolution is considered. Hence, the core of the partly decomposed micelles contained more than a single allophane particle. Upon extension of irradiation time to 30 min, most of the polymer was removed and ring-shaped features were detected on the substrate, as shown in the AFM topography image (Figure 6). The

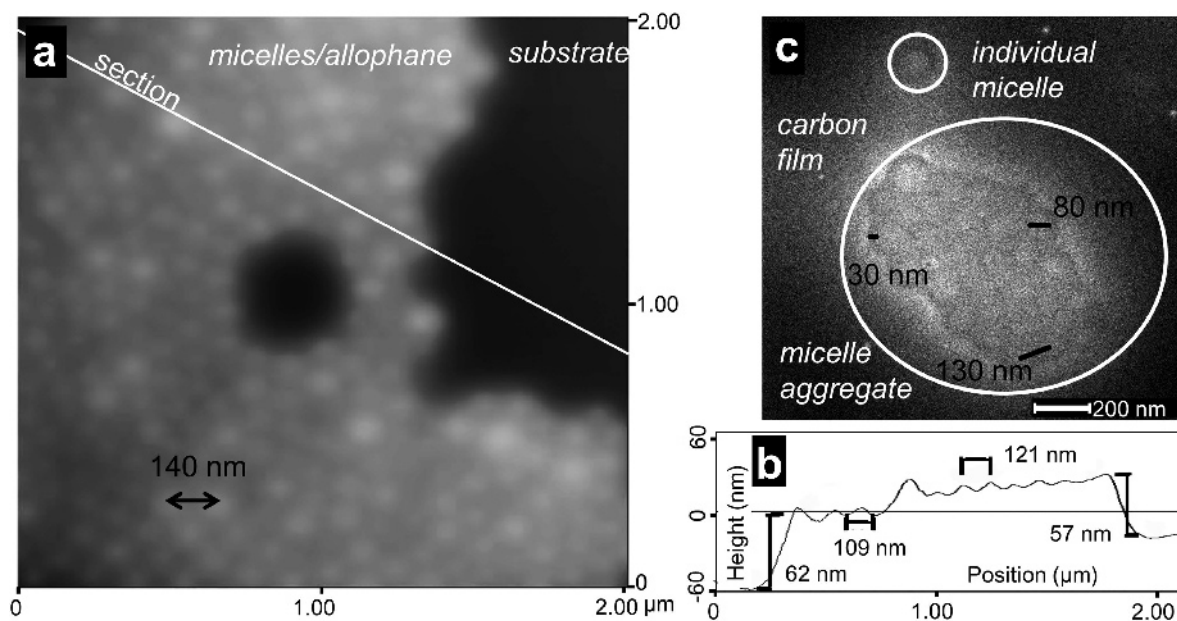


Figure 4. AFM topography image of PS–P2VP micelles containing allophane immobilized on a Si wafer surface. (a) Close packing of spheres is visible. (b) Cross-section along the white line in (a) showing the height of the polymer island in relation to the Si substrate, the center-to-center distance, and the diameter of the elevated structures formed by the particles. (c) TEM image of particle-containing micelles immobilized on the carbon film of a copper grid.

arrangement of the rings was similar to that of the particles with an average diameter of 15 nm as was revealed by AFM, which is in agreement with the

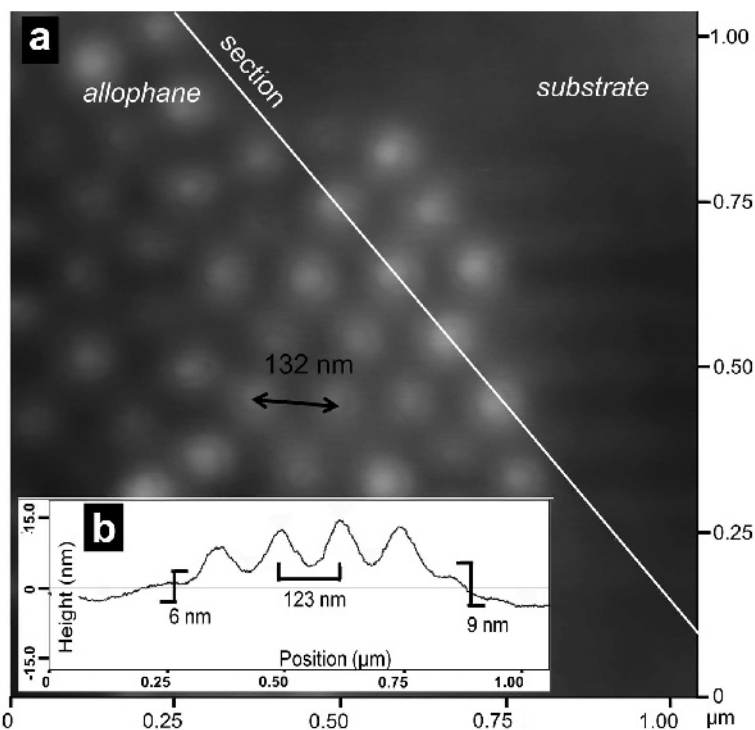


Figure 5. AFM topography image of allophane-containing micelles immobilized on a Si wafer surface after 10 min of UV treatment: (a) showing a close packing of spheres; (b) cross section along the white line in (a), showing the center-to-center distance of the allophanes and the height of the polymer island in relation to the Si substrate.

diameter of the particles deposited on the Si wafer from the aqueous suspension (Figure 3a). Consequently, the real particle diameter was  $\sim 5$  nm when taking into account tip convolution. The cross section (Figure 6c) along the white line shown in Figure 6b shows an average diameter of the ring-shaped features of 65 nm, which is in agreement with the dimensions determined for the polymer micelles (Figures 4 and 5), and a height of the ring wall of 5 nm, which is in agreement with the expected height of an allophane nanoparticle (Henmi and Wada, 1976). The difference in the measured particle heights (Figure 3b and Figure 6c) was probably due to thin polymer residues covering the Si substrate underneath the nanoparticles. These residues decreased the interaction between the substrate and the particles and thus prevented the allophanes from flattening. All these findings could be found reproducibly on different samples prepared in the same way.

### SUMMARY AND CONCLUSIONS

A method was presented to extract single, natural allophane nanoparticles from Japanese soil material in both aqueous and organic suspensions and to immobilize them on the surface of Si wafers. The advantage of applying an aqueous solution is that no amphiphilic polymer is needed and, hence, no contamination with organic residues occurs. Only a small surface density of particles was achieved, however, due to the poor tendency of the allophane particles to adhere to the Si substrate. By contrast, when suspending the allophane material in a solution of an amphiphilic diblock copolymer in toluene, micelles were formed, which contained allophane nanoparticles. Due to the attractive interaction between the outer sphere of the micelles and the Si wafer surface, the micelles were arranged in a

closely packed array, equidistant from each other, on the Si wafer surface, as a result of which allophane nanoparticles were transferred to the substrate. The advantage of this method is the formation of a consistent monolayer of self-assembled, particle-carrying micelles, which can be adjusted in size. After the polymer of the micelles was degraded by UV light, single allophane particles were immobilized on the surface and formed ring-like structures. This method not only increased the density of the allophane particles on the surface, but also resulted in a self-assembling structured deposition of the particles in comparatively few preparation steps. The method is reproducible and easy to scale up for the fabrication of nanostructured surfaces at low cost, as the particles originate from natural sources.

The results presented are a promising proof of concept for the application of allophane particles as building blocks for the preparation of self-assembled, nanostructured surfaces. Metals, such as gold, can also be used as a substrate for the immobilization. In this case a selective chemical, silane-based modification of the immobilized particles can be carried out to convert the oxidic particles, *e.g.* in bioadhesive nanodots, but without changing the chemical functionality of the substrate. The distance between the particles can be controlled by the chain length of the polymers. Although similar concepts for the application of other nanosized particles (*e.g.* gold or SiO<sub>2</sub>) exist, allophane nanoballs have the additional advantage that they are hollow spheres with variable pore size and with different chemical behavior of the inner and the outer sides of the shell. Such properties offer the opportunity to use allophane nanoballs as switchable nanocontainers for small molecules which can be released by an external trigger (*e.g.* pH value) with the advantage that those highly sophisticated nanodots are produced by nature.

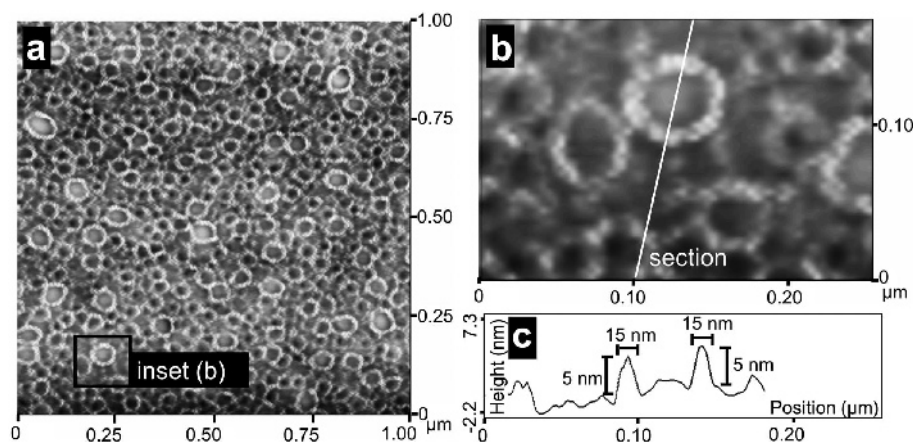


Figure 6. (a,b) AFM topography images of allophane particles on a Si wafer, at different magnifications. The substrate was prepared according to Figure 1 and was irradiated with UV light for 30 min. The polymer of the micelles containing allophane particles is removed and the allophane particles arrange as circles around the center of the destroyed micelles. (c) Cross section along the white line in (b). The height and width of the ring wall are in agreement with the dimensions of a single allophane nanoparticle.

## REFERENCES

- Abidin, Z., Matsue, N., and Henmi, T. (2007a) Nanometer-scale chemical modification of nano-ball allophane. *Clays and Clay Minerals*, **55**, 443–449.
- Abidin, Z., Matsue, N., and Henmi, T. (2007b) Differential formation of allophane and imogolite: experimental and molecular orbital study. *Journal of Computer-Aided Materials Design*, **14**, 5–18.
- Creton, B., Bougeard, D., Smirnov, K.S., Guilment, J., and Poncelot, O. (2008) Structural model and computer modeling study of allophane. *Journal of Physical Chemistry C*, **112**, 258–364.
- Glass, R., Arnold, M., Blümmel, J., Küller, A., Möller, M., and Spatz, J.P. (2008) Micro-nanostructured interfaces fabricated by the use of inorganic block copolymer micellar monolayers as negative resist for electron-beam lithography. *Advanced Functional Materials*, **13**, 569–575.
- Henmi, T. and Wada, K. (1976) Morphology and composition of allophane. *American Mineralogist*, **61**, 379–390.
- Higashi, T. and Ikeda, H. (1974) Dissolution of allophane by acid oxalate solution. *Clay Science*, **4**, 205–212.
- Karube, J., Nakaishi, K., Sugimoto, H., and Fujihira, M. (1996) Size and shape of allophane particles in dispersed aqueous systems. *Clays and Clay Minerals*, **44**, 485–491.
- Kaufhold, S., Kaufhold, A., Jahn, R., Brito, S., Dohrmann, R., Hoffmann, R., Gliemann, H., Weidler, P., and Frechen, M. (2009) A new massive deposit of allophane raw material in Ecuador. *Clays and Clay Minerals*, **57**, 72–81.
- Lipski, A.M., Jaquiere, C., Choi, H., Eberly, D., Stevens, M., Martin, I., Wei Chen, I., and Shastri, P. (2007) Nanoscale engineering of biomaterial surfaces. *Advanced Materials*, **19**, 553–557.
- Lohmueller, T., Bock, E., and Spatz, P. (2008) Synthesis of quasi-hexagonal ordered arrays of metallic nanoparticles with tuneable particle size. *Advanced Materials*, **20**, 2297–2302.
- Manzke, A., Pfahler, Ch., Dubbers, O., Plettl, A., Ziemann, P., Crespy, D., Schreiber, E., Ziener, U., and Landfester, K. (2007) Etching masks based on miniemulsions: a novel route towards ordered arrays of surface nanostructures. *Advanced Functional Materials*, **19**, 1337–1341.
- Nishikiori, H., Furukawa, M., and Fujii, T. (2011) Degradation of trichloroethylene using highly adsorptive allophane-TiO<sub>2</sub> nanocomposite. *Applied Catalysis B: Environmental*, **102**, 470–474.
- Ogaki, Y., Shinozuka, Y., Hara, T., Ichikuni, N., and Shimazu, S. (2011) Hemicellulose decomposition and saccharides production from various plant biomass by sulfonated allophane catalyst. *Catalysis Today*, **146**, 415–418.
- Onodera, Y., Iwasaki, T., Chatterjee, A., Ebina, T., Satoh, T., Suzuki, T., and Mimura, H. (2001) Bactericidal allophanic materials prepared from allophane soil. I. Preparation and characterization of silver/phosphorus–silver loaded allophanic specimens. *Applied Clay Science*, **18**, 123–134.
- Sikora, A. and Tuzar, Z. (2004) Association of two-block copolymer polystyrene-block-poly(2-vinylpyridine) in toluene. *Macromolecular Chemistry and Physics*, **184**, 2049–2059.
- Villarrubia, J.S. (1997) Algorithms for scanned probe microscope image simulation, surface reconstruction, and tip estimation. *Journal of Research of the National Institute of Standards and Technology*, **102**, 425–454.
- Vu, D.-H., Wang, K.-S., Nam, B.X., Bac, B.H., and Chu, T.-C. (2011) Preparation of humidity-controlling porous ceramics from volcanic ash and waste glass. *Ceramics International*, **37**, 2845–2853.
- Watanabe, K., Nakazawa, H., and Matsui, Y. (2009) Allophane films formed at the liquid/liquid interface. *Applied Clay Science*, **46**, 330–332.
- Woignier, T., Primera, J., Duffours, L., Dieudonné, P., and Raada, A. (2008) Preservation of the allophanic soils structure by supercritical drying. *Microporous and Mesoporous Materials*, **109**, 370–375.
- Xie, M. and Blum, F.D. (1996a) Dynamics of poly(styrene-b-2-vinylpyridine) in toluene. *Macromolecules*, **29**, 3862–3867.
- Xie, M. and Blum, F.D. (1996b) Adsorption and dynamics of low molecular weight poly(styrene-b-2-vinylpyridine) on silica and alumina in Toluene. *Langmuir*, **12**, 5669–5673.

(Received 6 February 2012; revised 7 July 2012; Ms. 651; AE: J.W. Stucki)